Available online at www.sciencedirect.com
ScienceDirect
Journal of Organometallic Chemistry 692 (2007) 79–87
Journal of Organometallic Chemistry
www.elsevier.com/locate/jorganchem

Synthesis, crystal structure, and coordination properties of a helical peptide having β-(3-pyridyl)-L-alanine and L-glutamic acid residues

Hiroyuki Oku [a,*], Yosuke Kimura [a], Mitsuo Ohama [b], Norikazu Ueyama [b], Keiichi Yamada [a], Ryoichi Katakai [a]

[a] *Department of Chemistry, Gunma University, Kiryu, Gunma 376-8515, Japan*
[b] *Department of Macromolecular Science, Graduate School of Science, Osaka University, Toyonaka, Osaka 560-0043, Japan*

Received 27 February 2006; received in revised form 20 March 2006; accepted 24 March 2006
Available online 3 September 2006

Abstract

A novel helical peptide containing β-(3-pyirdyl)-L-alanine (Pal) and L-glutamic acid (Glu) residues has been designed and successfully prepared as a model ligand of metalloenzyme active sites. The helical peptide, Boc-Leu-Aib-Glu-Leu-Leu-Pal-Aib-Leu-OEt (**1**) (Boc = *tert*-butoxycarbonyl, Aib = 2-aminoisobutylic acid) yields fine crystals as an acetnitrile solvate. The metal ion binding affinities of **1** were tested for $CoCl_2$ using UV/vis, CD, Raman, and ^1H NMR spectroscopies. The non-linear fitting calculations have revealed the 1:1 complex for $CoCl_2$ with the binding constant 3.6 (± 0.7) $\times 10^2$ M^{-1}.

Keywords: β-(3-pyridyl)-L-alanine; L-Glutamic acid; $CoCl_2$; Peptide; Helix; Crystal structure; Circular dichroism spectroscopy; Resonance Raman spectroscopy; Metalloenzyme; Active site

1. Introduction

Metalloenzymes such as ferritin and methane monooxygenase contain the coordination site and the recognition site for Fe ions on helical sequences. For example, Glu^{61} and His^{57} are on the same helix as estimated coordination ligands in a ferroxidase center of human mytochondrial ferritin of heavy chain subunit [1]. In the case of methane monooxygenase from *Methylosinus trichosporium* OB3b [2], two residues on the same helix, $Glu^{\alpha 243}$ and $His^{\alpha 246}$, bind an iron atom of the Fe_2O_2 diamond-core at the hydrophobic oxidation cavity.

Cobalt substitution have been widely reported for dinuclear iron proteins, such as hemerythrins [3], ribonucleotide reductase [4], methane monooxygenases [5], ferritines [6,7], and de novo enzymes [8,9]. Because Co(II) is very similar to Fe(II) both in ionic radious and charge and has d–d absorptions that can be a sensitive probe for the coordination geometry and the nature of the ligands [10]. Recent topics of cobalt derivatives are found for ferritins, which have been used for the nano-fabrication of cobalt-oxide nanoparticles through the oxidation reaction at the dinuclear metal ion center [11–13].

Continuing the study of enzyme active site models [14–16] and peptide crystals [17–21], we have planned to synthesize model complexes with a helical peptide to simulate these enzyme active sites. As an *N*-ligand, we have used β-(3-pyridyl)-L-alanine (Pal) instead of L-histidine (His). Pal is a non-coded amino acid, and is often used as an analog of His and phenylalanine (Phe) due to its structural similarity [22,23]. The reason why we have chosen Pal residue is the advantage for the peptide synthesis where the side chain of Pal does not require any protecting group. On the contrary, His requires an imidazole protection both on Boc- and Fmoc-chemistry and has been known as one of "difficult amino-acid residues". Thus, in this study, we have prepared a helical sequence having Pal and Glu residues to study the crystal structure and coordination reaction with $CoCl_2$ as a structural model of metalloenzyme active sites.

* Corresponding author. Tel./fax: +81 277 30 1343.
E-mail address: oku@chem.gunma-u.ac.jp (H. Oku).

0022-328X/$ - see front matter © 2006 Elsevier B.V. All rights reserved.
doi:10.1016/j.jorganchem.2006.03.051

2. Experimental

2.1. General procedures

Leucine and 1-ethyl-3-(3-dimethylaminopropyl) carbodiimide hydrochloride (EDC·HCl) were obtained from Nihon–Rikagaku–Yakuhin (Tokyo, Japan). Other reagents for peptide synthesis were obtained from Peptide Institute. Thin-layer chromatography (TLC) was carried out by using Kieselgel 60F254 aluminum plates obtained from Merck. Melting points were measured on a microanalytical melting point apparatus, YANACO MP-500P and were uncorrected. Optical rotations were measured on a JASCO DIP-1000 digital polarimeter (cell path length = 10 cm) at 20 °C. ^{1}H NMR spectra were taken on JEOL lambda-500 and JEOL AL-300 spectrometers using $CDCl_3$, dimethyl sulfoxide-d_6 (DMSO-d_6) and CD_3CN as solvents. UV/vis and CD spectra were recorded on a SHIMADZU UVPC-3100 and on a JASCO J-720, respectively.

2.2. Synthesis of peptide **1**

2.2.1. Synthetic procedure

The optically active Pal amino acid was prepared by hydrogenation of *N*-acetyl-β-(3-pyridyl)-α,β-dehydroalanine, which was obtained from *N*-acetyl-glycine and pyridine-3-aldehyde, followed by acylase-catalyzed enzymatic resolution [24–26]. Boc amino acids were prepared by standard procedure using di-*tert*-butyl dicarbonate, $(Boc)_2O$ [27,28].

The peptide **1** was prepared by stepwise elongation and fragment condensation starting from L-leucine ethyl ester hydrochloride (HCl·H-Leu-OEt). The scheme for the peptide synthesis was shown in Fig. 1. The coupling reactions were carried out using *N*,*N*′-dicyclohexylcarbodiimide (DCC) or 3-(3-dimethylaminopropyl)-1-ethylcarbodiimide hydrochloride (EDC·HCl) as a condensation reagent in purified chloroform or DMF as a solvent. 1-Hydroxybenzotriazole (HOBt) was used as an additive for coupling efficiency and to prevent racemization. The progress of each reaction was monitored by TLC with ninhydrin reaction. All the products were purified by recrystallization or column chromatography. The purity was confirmed by ^{1}H NMR and TLC. The final deprotection reaction for –OBzl group in the Glu residue was carried out by using 5% Pd–C/H_2 in MeOH at room temperature. Physicochemical data of the intermediates and the final product **1** were described below.

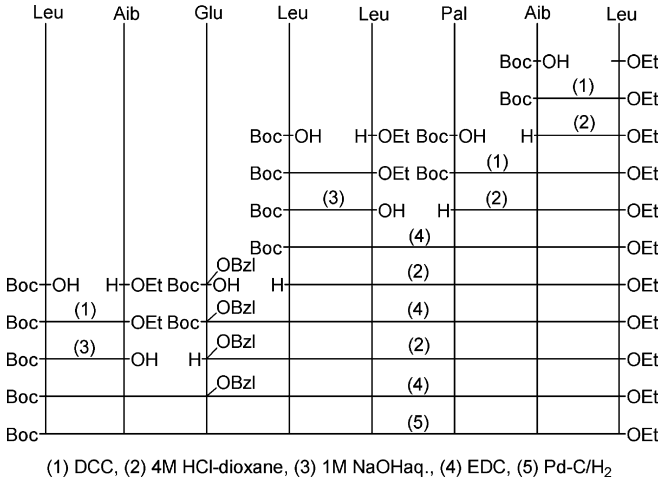

Fig. 1. Scheme for the synthesis of the peptide, **1**.

2.2.2. Boc-Aib-Leu-OEt (**2**)

Yield 65%, m.p. = 120–121 °C, $[\alpha]_D^{20} = -19.7°$ ($c = 0.1$, MeOH), $R_f = 0.70$ ($CHCl_3$–MeOH = 9:1 (=v/v)), ^{1}H NMR (300 MHz, $CDCl_3$, 25 °C) δ 6.81 (d, 1H), 4.86 (s, 1H), 4.54 (m, 1H), 4.14 (q, 2H), 1.71–1.52 (m, 3H), 1.48 (s, 3H), 1.45 (s, 3H), 1.41 (s, 9H), 1.24 (t, 3H), 0.91 (d, 6H).

2.2.3. Boc-Pal-Aib-Leu-OEt (**3**)

Yield 45%, m.p. = 141–142 °C, $[\alpha]_D^{20} = -25.6°$ ($c = 0.1$, MeOH), $R_f = 0.45$ ($CHCl_3$–MeOH = 9:1 (=v/v)), ^{1}H NMR (300 MHz, $CDCl_3$, 25 °C) δ 8.50 (q, 1H), 8.45 (d, 1H), 7.57 (m, 1H), 7.24 (q, 1H), 6.80 (d, 1H), 6.60 (s, 1H), 5.09 (d, 1H), 4.54 (m, 1H), 4.25–4.13 (m, 3H), 3.10 (q, 2H), 1.70–1.57 (m, 3H), 1.54 (s, 3H), 1.47 (s, 3H), 1.42 (s, 9H), 1.27 (t, 3H), 0.95 (d, 6H).

2.2.4. Boc-Leu-Pal-Aib-Leu-OEt (**4**)

Yield 75%, m.p. = 77–78 °C, $[\alpha]_D^{20} = -34.1°$ ($c = 0.1$, MeOH), $R_f = 0.28$ ($CHCl_3$–MeOH = 9:1 (=v/v)), ^{1}H NMR (300 MHz, $CDCl_3$, 25 °C) δ 8.45 (q, 1H), 8.43 (d, 1H), 7.59 (m, 1H), 7.24 (q, 1H), 6.87 (d, 1H), 6.82 (s, 1H), 6.74 (d, 1H), 4.91 (d, 1H), 4.55 (m, 2H), 4.17 (q, 2H), 3.99 (m, 2H), 3.14 (t, 2H), 1.76–1.52 (m, 6H), 1.50 (s, 3H), 1.47 (s, 3H), 1.40 (s, 9H), 1.28 (t, 3H), 0.96–0.88 (m, 12H).

2.2.5. Boc-Leu-Leu-Pal-Aib-Leu-OEt (**5**)

Yield 72%, m.p. = 92–93 °C, $[\alpha]_D^{20} = -49.7°$ ($c = 0.1$, MeOH), $R_f = 0.30$ ($CHCl_3$–MeOH = 9:1 (=v/v)), ^{1}H NMR (300 MHz, $CDCl_3$, 25 °C) δ 8.45 (q, 1H), 8.38 (d, 1H), 7.58 (m, 1H), 7.21 (m, 2H), 6.96 (s, 1H), 6.84 (d, 1H), 6.54 (d, 1H), 4.98 (d, 1H), 4.67–4.58 (m, 2H), 4.15 (m, 3H), 4.03 (m, 1H), 3.46 (d, 1H), 2.88 (q, 1H), 1.75–1.57 (m, 9H), 1.55 (s, 3H), 1.51 (s, 3H), 1.44 (s, 9H), 1.27 (t, 3H), 0.98–0.83 (m, 18H).

2.2.6. Boc-Glu(OBzl)-Leu-Leu-Pal-Aib-Leu-OEt (**6**)

Yield 70%, m.p. = 109–110 °C, $[\alpha]_D^{20} = -48.4°$ ($c = 0.1$, MeOH), $R_f = 0.44$ ($CHCl_3$–MeOH = 9:1 (=v/v)), ^{1}H NMR (300 MHz, $CDCl_3$, 25 °C) δ 8.34 (s, 2H), 7.58 (d, 1H), 7.36 (s, 5H), 7.24–7.13 (m, 3H), 7.02 (s, 1H), 6.92 (d, 1H), 6.70 (d, 1H), 6.23 (d, 1H), 5.15 (s, 2H), 4.76–4.66 (m, 2H), 4.21 (m, 1H), 4.12–4.05 (m, 3H), 3.89 (m, 1H), 3.54 (d, 1H), 2.79 (t, 1H), 2.55 (m, 2H), 2.06 (m, 2H), 1.79–1.68 (m, 9H), 1.58 (s, 3H), 1.52 (s, 3H), 1.48 (s, 9H), 1.20 (t, 3H), 0.97–0.79 (m, 18H).

2.2.7. Boc-Leu-Aib-Glu(OBzl)-Leu-Leu-Pal-Aib-Leu-OEt (7)

Yield 50%, m.p. = 171–173 °C, $[\alpha]_D^{20} = -6.0°$ ($c = 0.1$, MeOH), $R_f = 0.41$ ($CHCl_3$–MeOH = 9:1 (=v/v)), ^1H NMR (300 MHz, $CDCl_3$, 25 °C) δ 8.47 (s, 1H), 8.40 (d, 1H), 7.84 (d, 2H), 7.66 (d, 1H), 7.34–7.27 (m, 7H), 7.16 (m, 3H), 6.88 (d, 1H), 5.15 (s, 3H), 4.70–4.63 (m, 2H), 4.21–3.92 (m, 6H), 3.57 (d, 1H), 2.79 (t, 1H), 2.58 (m, 2H), 2.14 (m, 2H), 1.83–1.61 (m, 12H), 1.59 (s, 3H), 1.56 (s, 3H), 1.47 (s, 3H), 1.43 (s, 9H, CH), 1.41 (s, 3H), 1.20 (t, 3H), 0.99–0.80 (m, 24H).

2.2.8. Boc^0-Leu^1-Aib^2-Glu^3-Leu^4- Leu^5-Pal^6-Aib^7-Leu^8-OEt^9 (1)

Yield 98%, m.p. = 122–123 °C, $[\alpha]_D^{20} = -33.5°$ ($c = 0.1$, MeOH), $R_f = 0.13$ ($CHCl_3$–MeOH-CH_3COOH = 25:5:1 (=v/v/v)). ESI-MS (m/z) calcd for $C_{52}H_{87}N_9O_{13}$:1045.6. Found, 1046.8 ($[M + H]^+$). ^1H NMR (500 MHz, CD_3CN, 25 °C): for Boc^1, δ 1.44 (s, 9H); for Leu^2, 5.89 (d, $^3J_{NHC\alpha} = 4.6$ Hz, 1H, NH), 3.90 (1H, $C^{\alpha}H$), 1.67 (2H, $C^{\beta}H$), 1.50 (1H, $C^{\gamma}H$), 0.95 (3H, $C^{\delta}H$), 0.91 (3H, $C^{\delta}H$); for Aib^3, 7.64 (s, 1H, NH), 1.42 (6H, $C^{\beta}H$); for Glu4, 7.79 (d, $^3J_{NHC\alpha} = 3.0$ Hz, 1H, NH), 4.05 (1H, $C^{\alpha}H$), 2.08 (1H, $C^{\beta}H$), 2.00 (1H, $C^{\beta}H$), 2.45 (2H, $C^{\gamma}H$); for Leu^5, 7.83 (d, $^3J_{NHC\alpha} = 5.3$ Hz, 1H, NH), 4.15 (1H, $C^{\alpha}H$), 1.83 (2H, $C^{\beta}H$), 1.56 (1H, $C^{\gamma}H$), 0.97 (3H, $C^{\delta}H$), 0.91 (3H, $C^{\delta}H$); for Leu^6, 7.48 (d, $^3J_{NHC\alpha} = 5.3$ Hz, 1H, NH), 3.96 (1H, $C^{\alpha}H$), 1.57 (2H, $C^{\beta}H$), 1.28 (1H, $C^{\gamma}H$), 0.83 (3H, $C^{\delta}H$), 0.75 (3H, $C^{\delta}H$); for Pal^7, 8.49, 7.73, 7.21, 8.39 (pyridine ring of C^2H, C^4H, C^5H, C^6H, respectively), 7.15 (d, $^3J_{NHC\alpha} = 9.1$ Hz, 1H, NH), 4.48 (1H, $C^{\alpha}H$), 3.47 (1H, $C^{\beta}H$), 2.72 (1H, $C^{\beta}H$), 1.50 (1H, $C^{\gamma}H$), 0.95 (3H, $C^{\delta}H$), 0.91 (3H, $C^{\delta}H$); for Aib^8, 7.64 (s, 1H, NH), 1.42 (6H, $C^{\beta}H$); for Glu^4, 7.79 (d, $^3J_{NHC\alpha} = 3.0$ Hz, 1H, NH), 4.05 (1H, $C^{\alpha}H$), 2.08 (1H, $C^{\beta}H$), 2.00 (1H, $C^{\beta}H$), 2.45 (2H, $C^{\gamma}H$); for Leu^9, 7.83 (d, $^3J_{NHC\alpha} = 5.3$ Hz, 1H, NH), 4.15 (1H, $C^{\alpha}H$), 1.83 (2H, $C^{\beta}H$), 1.56 (1H, $C^{\gamma}H$), 0.97 (3H, $C^{\delta}H$), 0.91 (3H, $C^{\delta}H$); for OEt^9, 4.07 (2H, $-CH_2-$), 1.17 (3H, $-CH_3$).

2.3. X-ray crystallography

To obtain single crystals suitable for diffraction analysis, for example, 10 mg of **1** was dissolved in 0.5 mL of warm acetnitrile and completely dissolved, resulting in fine platelet crystals of **1**·CH_3CN after 3 h and kept for 12 h at 15 °C. X-ray diffraction data were collected on a Rigaku R-AXIS RAPID imaging plate area detector with monochromated Cu $K\alpha$ radiation, $\lambda = 1.5418$ Å at −100 °C. We have successfully solved the structure of **1**·CH_3CN by a direct method for macromolecular crystals, Sir2002 [29]. An empirical absorption collection program, DIFABS [30] was applied which resulted in transmission factors ranging from 0.76 to 1.07. Non-hydrogen atoms were refined with anisotropic displacement tensors. H-atoms except at the carboxyl group –OH of Glu^3 were located in calculated positions and refined with a riding model. The carboxyl –OH was clearly found in a difference Fourier map and refined with a riding model as well.

Crystal and refinement data for **1**·CH_3CN ($C_{54}H_{87}N_{10}O_{13}$): $P2_12_12_1$ (#19, orthorhombic), $a = 10.525(1)$ Å, $b = 21.969(2)$ Å, $c = 27.091(3)$ Å, $V = 6263.9$ (13) Å^3, $Z = 4$, $D_{calc} = 1.513$ g/cm^3, measured reflections = 55 699, unique reflections = 6323 ($R_{int} = 0.079$), $R_1 = 0.069$, $wR_2 = 0.069$, goodness of fit = 0.86.

3. Results

3.1. Peptide design and synthesis

To make a helical structure, we have chosen Leu and Aib residues, which is generally considered as helix-forming units [17–19,31–33]. The α,α-disubstituted amino acid, Aib, is a sterically hindered amino acid and was used as a conformational constraint [34,35] and thus suitable for the stable formation of helical structures. Leu and Aib residues are also suitable to make a soluble helix to various organic solvents [31]. Especially in a Leu based helix, the whole molecule is completely covered with iso-butyl side chains of Leu residues [17–19,31]. When designing our helical sequence, two metal ion-binding residues, Glu and Pal, were inserted into the positions where both carboxyl- and pyridyl-groups are facing each other in an ideal helical rod, such as -Glu-Leu-Leu-Pal-. Based on these structural considerations, we have prepared an 8-mer sequence, Boc-Leu-Aib-Glu-Leu-Leu-Pal-Aib-Leu-OEt (**1**), according to the synthetic scheme (Fig. 1). The amino- and the carobxy-terminous are both capped with a Boc- and an ethyl ester, respectively for the helix stabilization and the solubility to organic solvents. The obtained product, **1** successfully shows fine crystallinity and solubility as expected by the molecular design.

3.2. Crystal structure of 1

Single crystals of **1** suitable for X-ray crystallography was successfully obtained from a CH_3CN solution as shown in Fig. 2a. A solution of CH_3OH or $CHCl_3$ only yielded colorless powders not suitable for the diffraction study. Fig. 2b and c show the stereo drawing of **1** and a packing diagram, respectively. The crystal structure has revealed that a pyridyl- and a carboxyl-group are located on the same side of the helical rod. Therefore this sequence is suitable for the metal ion chelation on the same helix.

The torsion angles of main and side chains are listed in Table 1. The ϕ and ψ torsional angles of the helical residues from Leu^1 to Leu^5 have shown similar pairs of angles except an Aib^2 residue ranging from −61.3 to −65.6° and −19.9 to − 26.3°, respectively. In the Aib^2 residue, the ϕ and ψ values (−54.8°, −23.0°) very close to the helical part of Leu^1–Leu^5. As a whole, the backbone torsion angles for residues from Leu^1 to Leu^5 lie in the right handed 3_{10} helix region and not α-Helix in a Ramachandran plot [36–39]. For the side chains of Leu residues, the torsion angles of

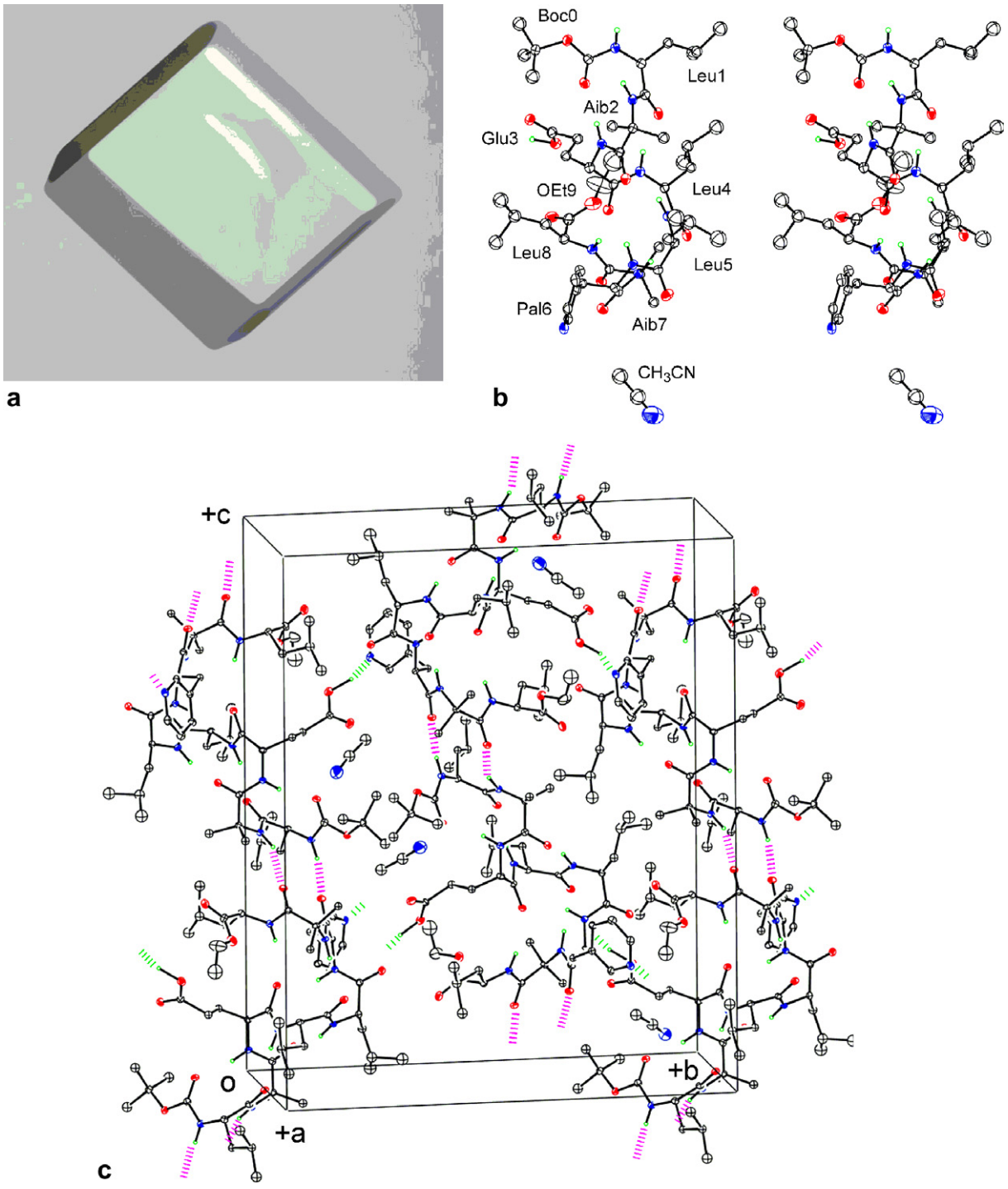

Fig. 2. (a) A polarized light photograph of a crystal of **1**, about 3 mm on a side. (b) Stereo drawing of **1** with 50% thermal ellipsoids. All hydrogen atoms except NHs are omitted for clarity. (c) A packing diagram of **1**. Intermolecular (purple) and intramolecular (green) hydrogen bonds are indicated as dotted lines (For interpretation of the references to color in this figure legend, the reader is referred to the web version of this article.).

Leu[4] and Leu[5], which are located in the middle of the helix, have suggested a stable orientation, $g^-(t,g^-)$ [40–43]. The rest of Leu residues, the chain head Leu[1] and the chain end Leu[8] adopt the other stable form, $t(g^+,t)$. Similar conformational tendencies for the Leu side chain have been observed for an 11-residue helix, Boc-Leu-Leu-Ala-(Leu-Leu-Lac)$_3$-Leu-Leu-OEt [17]. In this helix, the chain head and the chain end Leu adopt the same $t(g^+,t)$ conformation. The rest of Leu residues show $g^-(t,g^-)$ as observed in the middle of the helix of **1**. Therefore these pairs of χ_1 and χ_2 parameters are probably favourable for the L-leucine based right-handed helices.

The intramolecular and intermolecular hydrogen bonds are listed in Table 2. A total of seven intramolecular hydro-

Table 1
Torsion angles (°) for Boc^0-Leu^1-Aib^2-Glu^3-Leu^4-Leu^5-Pal^6-Aib^7-Leu^8-OEt^9 (**1**)

Residues	Angles				
	ϕ	ψ	ω	$\chi1$	$\chi2$
Boc^0			−173.3(5)		
Leu^1	−63.7(7)	−26.3(8)	176.8(5)	−167.1(6)	59.4(8)
					179.2(6)
Aib^2	−54.8(7)	−23.0(8)	179.7(5)		
Glu^3	−61.3(7)	−19.9(8)	−176.5(5)	76.1(7)	171.7(5)
Leu^4	−65.6(7)	−20.9(8)	174.7(5)	−76.0(7)	−61.5(9)
					−179.0(6)
Leu^5	−62.0(8)	−22.6(9)	−178.9(5)	−77.3(8)	−68(1)
					173.2(7)
Pal^6	−102.4(7)	1.8(8)	−173.0(5)	−71.4(7)	
Aib^7	−50.6(7)	41.0(7)	170.7(5)		
Leu^8	−71.3(7)	−32.4(9)	−176.0(6)	−171.8(7)	−61(1)
					−176.9(7)

The torsion angles for rotation about bonds of the peptide backbone (ϕ, ψ, and ω) and about bonds of the amino acid side chains ($\chi1$, $\chi2$) are described in Ref. [30].

gen bonds are found for carbonyl oxygens and amide NHs and dotted as purple lines shown in Fig. 2c. Four of these interactions are of (i, $i+3$) types that form a 3_{10} helical structure from Leu^1 to Leu^5. The bond length of N···O are well corresponded to the reported data for 3_{10}-helices in native proteins [44,45] and in synthetic peptides containing Aib residues [46,47]. Other intramolecular interactions are found for the residues of (Glu^3, Leu^8) and (Leu^4, Aib^7) that form a turn structure from Glu^3 to OEt^9. The hydrogen bond between Leu^4 C═O and Aib^7 NH is a typical type I β-turn [48] where the pair of (ϕ, ψ) for Leu^5 and Pal^6 are (−62.0°, −22.6°) and (−102.4°, 1.8°), respectively.

For intermolecular interactions, two hydrogen bonds of NH···O═C connect the peptide helices into infinite chains along c-axis. In Fig. 2c, three molecular columns are shown in this unit cell. The green dotted lines indicate these intermolecular hydrogen bonds. The connecting residues are found at the head to tail positions, Leu^1 to Pal^6 and Aib^2 toAib^7. Interestingly the columns are connected each other by an intermolecular hydrogen bond connecting the side chains of Glu^3 carboxyl- and Pal^6 pyridyl-group, –OH···N.

The X-ray structural analysis of **1** is summarized as follows: the octapeptide begins with the 3_{10}-helix from Leu^1 to Lac^5 followed by the type I β-turn from Leu^4 to Aib^7, and ends with the other reverse turn from Glu^3 to Leu^8. The shape of the whole molecule resembles a hydrophobic rod with an end-cap. Complete covering of the polar peptide main chain with hydrophobic alkyl side chains clearly contribute to form a stable helical structure to hide amide moieties in the main-chain and thus soluble to various organic solvents.

3.3. Metal ion binding studies of *1* with $CoCl_2$

3.3.1. Visible spectra

We have monitored the binding properties between **1** and $CoCl_2$ by using a spectral change of visible spectra (Fig. 3a). In this titration study, the condensed solution of **1** was gradually added into the 0.1 mM of $CoCl_2$ solution in CH_3CN at 20 °C. Upon addition $CoCl_2$, the intensity of the absorption maximum of at 570, 614, and 684 nm, assignable to d–d transitions of Co(II) ion, decreased in intensity through many isosbestic points at 552, 578, 600, 632, and 662 nm. After the addition of enough ligand peptide **1**, new maxima found at 589 and 675 nm.

Plots of the decrease in the absorbance at 684 nm will reach slowly to the saturation when the excess amount of peptide is added to the solution as shown in Fig. 3b. The non-linear fitting analysis [49] applied for these data points has indicated a 1:1 complexation with the formation constant (K) of 3.6 (±0.7) × 10^2 M^{-1} [50]. The Job plot showed a maximum value for the absorbance at 684 nm when the mole fraction of **1** reached 0.5, thereby supporting a 1:1 binding between the peptide and $CoCl_2$ (Fig. 4). Interestingly, a kink was observed for the Job plot at 0.7 mole fraction. This suggests the existence of smaller amount of a 3:2 or 2:1 complex for **1** and $CoCl_2$. In the case of $FeCl_2$ species, a 3:2 association was dominantly formed in the same reaction system.

The Job plot result has suggested the tiny existence of a peptide:metal = 3:2 or 2:1 complex. However, it seems curious why the titration result was successfully analyzed based on a 1:1 complex formation. Actually the non-linear fitting analysis based on 3:2 complexes has also resulted the

Table 2
Intramolecular and intermolecular hydrogen bond geometries (Å, °) for Boc^0-Leu^1-Aib^2-Glu^3-Leu^4-Leu^5-Pal^6-Aib^7-Leu^8-OEt^9 (**1**)

Acceptor C═O	Donor NH	O···N	H···O	N···H···O	Type (assignment)
O102 (Boc^0)	N131 (Pal^3)	3.006(6)	2.075	166.0	i, $i+3$ (3_{10} helix)
O111 (Leu^1)	N141 (Leu^4)	2.974(6)	2.042	166.5	i, $i+3$ (3_{10} helix)
O121 (Aib^2)	N151 (Leu^5)	2.930(6)	2.048	153.7	i, $i+3$ (3_{10} helix)
O131 (Glu^3)	N161 (Pal^6)	3.035(6)	2.175	149.9	i, $i+3$ (3_{10} helix)
O131 (Glu^3)	N181 (Leu^8)	3.402(6)	2.472	166.1	i, $i+5$ (reverse turn)
O141 (Leu^4)	N171 (Aib^7)	3.090(6)	2.161	165.7	i, $i+3$ (type I β-turn)
O161 (Pal^6)	N111 (Leu^1)	2.928(6)	1.994	167.1	Head to tail
O171 (Aib^7)	N121 (Aib^2)	3.032(6)	2.175	152.6	Head to tail
N166 (Pyridyl group of Pal^6)	O136 (Carboxyl group of Glu^3)	2.696(7)	1.489	158.5	Side chain to side chain

Hydrogen atoms were placed at idealized positions with N–H = 0.95 Å.

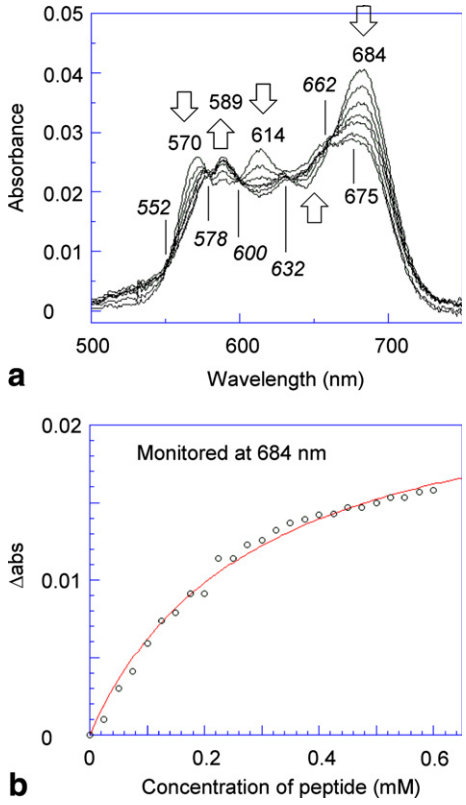

Fig. 3. (a) Absorption spectral changes for $CoCl_2$ with the titration of **1** in CH_3CN ($[CoCl_2] = 0.10$ mM, at 20 °C). (b) Absorption changes at 684 nm. Data were analyzed by non-linear curve fitting analysis, $K = [CoCl_2\text{-peptide}]/[CoCl_2][peptide]$. The calculated results are $\Delta Abs^{\infty} = 0.0238$ (± 0.0020) and $K = 3.6\ (\pm 0.7) \times 10^2\ M^{-1}$.

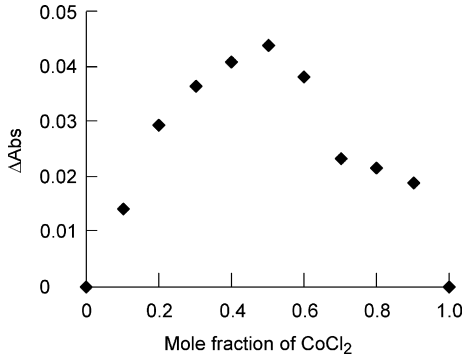

Fig. 4. Job plot for **1** and $CoCl_2$ in CN_3CN, monitored at Co(II) absorption at 684 nm ($[Peptide] + [CoCl_2] = 0.10$ mM at 20 °C).

formation constant (K) of 4.6 (± 0.5) $\times 10^2\ M^{-2/3}$ [50], although the 3:2 species is only dominant at the peptide-rich environment.

3.3.2. Circular dichroism spectra

Circular dichroism spectra are shown in Fig. 5 for the model peptide **1** in the absence (solid line) and the presence of metal ion, $CoCl_2$ (dotted lines) in CN_3CN at 20 °C ($[peptide] = 1.0$ mg/mL). The CD spectrum of **1** exhibited a positive maximum at 192nm and a negative maximum at 206 nm, indicating the formation of helical structure. Only tiny negative shoulder was observed at 222 nm, which is typically observed for an α-helical structure [51–53]. By the addition of $CoCl_2$ species to the solution of **1**, the continuous spectral change in intensity are observed for both CD bands at 191 and 206 nm. This intensity changing of the spectra suggested the slight conformational stabilization of the peptide, probably the increasing the helical structure among the total conformational ensemble, upon interaction with $CoCl_2$.

3.3.3. ^1H NMR spectra

Changes in the ^1H NMR spectrum of **1** before and after the addition of $CoCl_2$ in CD_3CN at 20 °C are shown in Fig. 6. The sample solution of **1** was prepared in a 5 mm NMR gastight tube, followed by the 0.25, 0.50, 1.0, 2.0 equivalent of $CoCl_2$ in each spectral measurement. As shown in Fig. 6b, the signals of the pyridyl group CHs (7.0–8.5 ppm), Pal^6 $C_\beta H_2$ (2.7 and 3.4 ppm) and Glu^3 $C_\gamma H_2$ (2.45 ppm) are disappeared in the presence of only 0.25 equivalent of $CoCl_2$. The disappearance has indicated the coordination to both side chains of Glu^3 and Pal^6 residues. The resonance signals due to amide NHs which appeared in the range of 5.5–8.0 ppm, became weak and broad upon addition of the metal chloride. Those broaden signals are gradually shifted low field by increasing the amount of $CoCl_2$. Similarly the signals due to Pal^6, Leu^1, Leu^4, Leu^5, Leu^8, and Glu^3 $C_\alpha Hs$, which appeared at 3.5–4.6 ppm changed to broad multiplets.

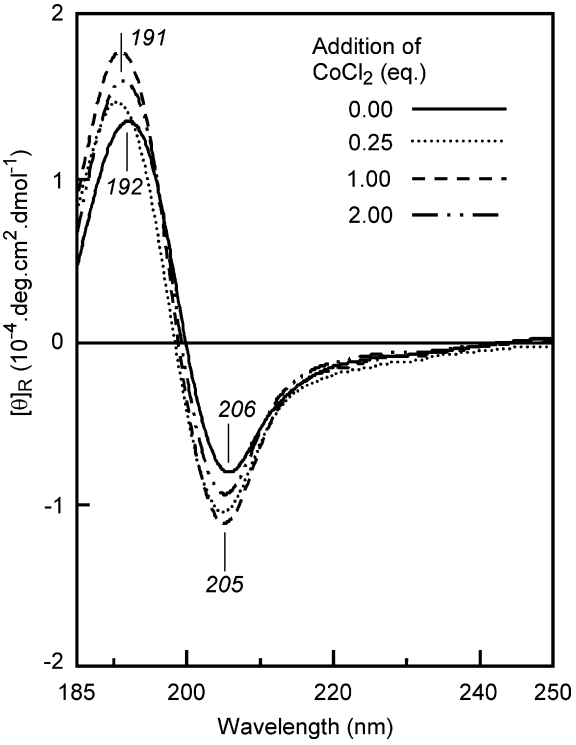

Fig. 5. CD spectral changes of **1** by the addition of $CoCl_2$ in CH_3CN ($[\mathbf{1}] = 1.0$ mM, at 20 °C).

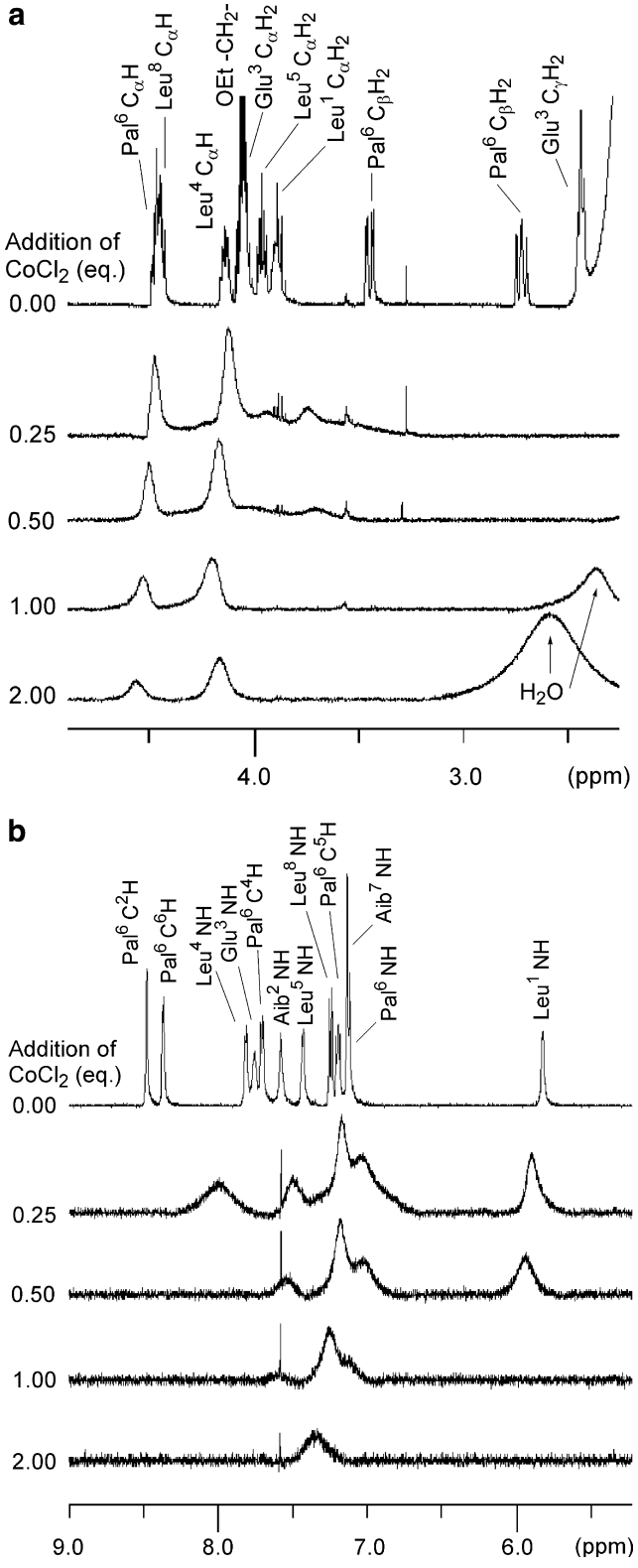

Fig. 6. ^{1}H NMR spectral changes of **1** by the titration of $CoCl_2$ in CD_3CN ([**1**] = 3.7 mM, at 20 °C). The spectra of (a) CH signals and (b) amide NHs and pyridyl groups are shown.

These broaden spectra are indications of the slow exchange rate between the free species of **1** and $CoCl_2$ and the complex at 20 °C.

3.3.4. Raman spectra

Fig. 7a and b show the Raman spectra of the concentrated oil from a CH_3CN solution containing equivalent mol of **1** and $CoCl_2$ with 632.8 and 514.5 nm laser excitation, respectively. The absorption spectra of this reaction mixture have absorption maxima at around 570–690 nm that are due to d–d transition bands of Co(II) as shown in Fig. 3. Therefore the wavenumbers at 632.8 and 514.5 nm are located on the middle region and an absorption edge of the d–d spectra, respectively. With the 632.8 nm laser, the Raman spectra have shown the enhancements at 311, 283, and 208 cm^{-1}. These bands can be assignable to the ν_{as}(Co–Cl), ν_s(Co–Cl), and ν(Co–N) stretchings [54,55], respectively, if the complex have a tetrahedral coordination core of $Co^{II}Cl_2NO$. Significant band was not observed for ν(Co–O) stretching that probably dose not show strong enhancement in resonance Raman effect due to the mostly ionic and scarcely covalent character of the carboxylato coordination. Relatively weak but significant bands were observed at 1451 and 1036 cm^{-1} that are associated to the carboxylate and pyridine coordinations to the Co(II) atom. In the case of 514.5 nm excitation, only weak shoulders were observed in the region, 350–200 cm^{-1}. This is clearly due to the weak visible absorption of the d–d transition bands associated with mainly metal d-orbitals and covalent contribution from ligand p-orbitals. On the contrary, numerous bands were observed in the range 600–1500 cm^{-1}. Among them, the band at 1451, 1420, 1036 cm^{-1} are assignable to carboxylate, amide III, pyridyl group, respectively.

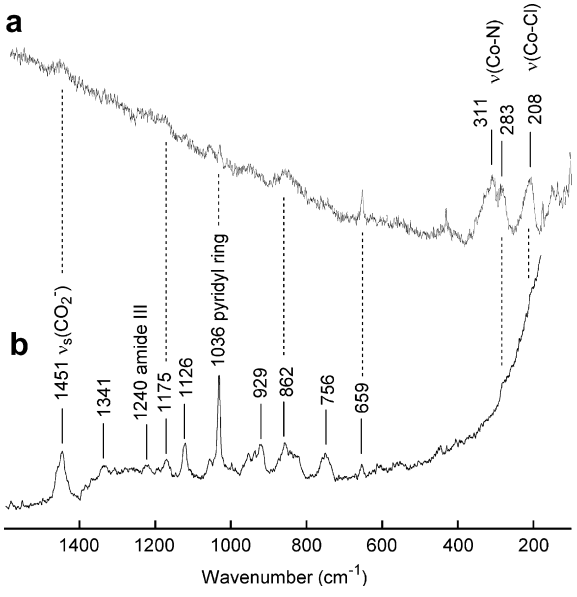

Fig. 7. Raman spectra for the *in situ* formed peptide complex between **1** and $CoCl_2$ (concentrated from CH_3CN solution, [**1**] = [$CoCl_2$] = 2 mM) with 514.5 and 632.8 nm laser excitation.

4. Conclusion

We have described the preparation of a helical sequence, **1**, which contains Pal and Glu residues by solution-phase synthesis. The successful analysis by X-ray diffraction has revealed that the peptide have 3_{10}-helical structure in solid state, because of its short sequence and the containing two Aib residues. The titration study of **1** has shown relatively weak chelating ability with $CoCl_2$ as observed in ^1H NMR and visible spectra, although the Raman spectra have strongly suggested the peptide coordination with a Co(II) atom. We are now extending our study to histidine peptides and other metal ions such as $FeCl_2$ toward the total chemical syntheses of metallo-enzyme active sites by combining X-ray crystallographic analysis.

5. Deposited material

Crystallographic data for the structure reported in this paper have been deposited with the Cambridge Crystallographic Data Centre as CCDC 299275. Copies can be obtained free of charge on application to CCDC, 12 Union Road, Cambridge CB2 1EZ (Fax: international +44(0) 1223/336-033; E-mail: deposit@ccdc.com.ac.uk). Tables of crystallographic data, atomic parameters and geometric parameters are available as Supplementary data.

Acknowledgements

HO thanks Grant-in-Aid for Scientific Research on Priority Areas (No. 14078101 and 16033211, Reaction Control of Dynamic Complexes) from Ministry of Education Culture, Sports, Science and Technology, Japan.

Appendix A. Supplementary data

Supplementary data associated with this article can be found, in the online version, at doi:10.1016/j.jorganchem.2006.03.051.

References

[1] For example of human heavy-chain subunit structure: PDB code, 1R03; B. Langlois d'Estaintot, P. Santambrogio, T. Granier, B. Gallois, J.M. Chevallier, G. Precigoux, S. Levi, P. Arosio, J. Mol. Biol. 340 (2004) 277–293.
[2] For example of methane monoxygenase structure: PDB code, 1MHY; N. Elango, R. Radhakrishnan, W.A. Froland, B.J. Wallar, C.A. Earhart, J.D. Lipscomb, D.H. Ohlendorf, Protein Sci. 6 (1997) 556–568.
[3] J.J. Zhang, D.M. Kurtz Jr., M.J. Maroney, J.P. Whitehead, Inorg. Chem. 31 (1992) 1359–1366.
[4] T.E. Elgren, L.-J. Ming, L. Que Jr., Inorg. Chem. 33 (1994) 891–894.
[5] M.H. Sazinsky, M. Merkx, E. Cadieux, S. Tang, S.J. Lippard, Biochemistry 43 (51) (2004) 16263–16276.
[6] A.M. Keech, N.E. Le Brun, M.T. Wilson, S.C. Andrews, G.R. Moore, A.J. Thomson, J. Biol. Chem. 372 (1997) 422–429.
[7] N.E. Le Brun, A.M. Keech, M.R. Mauk, A.G. Mauk, S.C. Andrews, A.J. Thomson, G.R. Moore, FEBS Lett. 397 (1996) 159–163.
[8] S. Geremia, L. Di Costanzo, L. Randaccio, D.E. Engel, A. Lombardi, F. Nastri, W.F. DeGrado, J. Am. Chem. Soc. 127 (2005) 17266–17276.
[9] C.M. Summa, M.M. Rosenblatt, J.K. Hong, J.D. Lear, W.F. DeGrado, J. Mol. Biol. 321 (2002) 923–938.
[10] L. Banci, A. Bencini, C. Benelli, D. Gatteschi, C. Zanchini, Struct. Bonding 52 (1982) 37–86.
[11] B. Zhang, J.N. Harb, R.C. Davis, J.W. Kim, S.H. Chu, S. Choi, T. Miller, G.D. Watt, Inorg. Chem. 44 (2005) 3738–3745.
[12] H.A. Hosein, D.R. Strongin, M. Allen, T. Douglas, Langmuir 20 (2004) 10283–10287.
[13] M. Allen, D. Willits, M. Young, T. Douglas, Inorg. Chem. 42 (2003) 6300–6305.
[14] H. Oku, N. Ueyama, A. Nakamura, Inorg. Chem. 36 (1997) 1504–1516.
[15] H. Oku, N. Ueyama, A. Nakamura, Bull. Chem. Soc. Jpn. 72 (1999) 2261–2270.
[16] R. Nakai, H. Oku, K. Yamada, R. Katakai, in: T. Yamada (Ed.), Peptide Science 2002, The Japanese Peptide Society, Osaka, 2003, pp. 313–317.
[17] H. Oku, T. Ohyama, A. Hiroki, K. Yamada, K. Fukuyama, H. Kawaguchi, R. Katakai, Biopolymers 54 (2004) 375–378.
[18] T. Ohyama, H. Oku, Y. Yoshida, R. Katakai, Biopolymers 58 (2001) 636–642.
[19] T. Ohyama, H. Oku, A. Hiroki, Y. Maekawa, Y. Yoshida, R. Katakai, Biopolymers 75 (2000) 242–254.
[20] H. Oku, T. Endo, K. Yamada, R. Katakai, Acta Crystallogr., Sect. E 61 (2005) o3864–o3866.
[21] H. Oku, K. Kuriyama, K. Omi, K. Yamada, R. Katakai, Acta Crystallogr., Sect. E 61 (2005) o3867–o3869.
[22] D.L. Heyl, M. Dandabathula, K.R. Kurtz, C. Mousigian, J. Med. Chem. 38 (1995) 1242–1246.
[23] Y. Levin, R.K. Khare, G. Abel, D. Hill, E. Eriotou-Bargiota, J.M. Becker, F. Naider, Biochemistry 32 (1993) 8199–8206.
[24] P.N. Rao, J.E. Burdett Jr., J.W. Cessac, C.M. Dinunno, D.M. Peterson, H.K. Kim, Int. J. Peptide Protein Res. 29 (1987) 118–125.
[25] K. Folkers, T. Kubiak, J. Stepinski, Int. J. Peptide Protein Res. 24 (1984) 197–200.
[26] C. Döbler, H.-J. Kreuzfeld, M. Michalik, H.W. Krause, Tetrahedron: Asymmetr. 7 (1996) 117–125.
[27] D.S. Tarbell, T. Yamamoto, B.M. Pope, Proc. Natl. Acad. Sci. USA 69 (1972) 730–732.
[28] L. Moroder, A. Hallet, E. Wunsch, O. Keller, G. Wersin, Hoppe-Seyler's Z. Physiol. Chem. 357 (1976) 1651–1653.
[29] M.C. Burla, M. Camalli, B. Carrozzini, G.L. Casarano, C. Giacovazzo, G. Polidori, R. Spagna, J. Appl. Crystallogr. 36 (2003) 1103.
[30] N. Walker, D. Stuart, Acta. Cryst. A 39 (1983) 158–166.
[31] R. Katakai, K. Kobayashi, N. Yonezawa, M. Yoshida, Biopolymers 38 (1995) 285–290.
[32] R. Katakai, Y. Nakayama, J. Chem. Soc., Chem. Commun. (1977) 805–806.
[33] G.D. Fasman, Poly Amino Acids, Marcel Dekker, New York, 1967, pp. 499.
[34] C. Toniolo, M. Crisma, F. Formaggio, C. Peggion, Biopolymers. (Pept. Sci.) 60 (2001) 396–419.
[35] M. Hanyu, D. Ninoura, R. Yanagihara, T. Murashima, T. Miyazawa, T. Yamada, J. Pept. Sci. 11 (2005) 491–498.
[36] R.E. Dickerson, I. Geis, The structure and Action of Proteins, Benjamin/Cummings Publishing Company, Menlo Park, 1969, pp. 24–43.
[37] α-Helix, $(\phi, \psi) = (-57°, -47°)$: S. Arnott, A.J. Wonacott, J. Mol. Biol. 21 (1966) 371–383.
[38] Aib based 3_{10} helix, $(\phi, \psi) = (-60°, -30°)$: C. Toniolo, E. Benedetti, Trends Biochem. Sci. 16 (1991) 350–353.
[39] 3_{10}-Helices in proteins, $(\phi, \psi) = (-71°, -18°)$: D.J. Barlow, J.M. Thornton, J. Mol. Biol. 201 (1988) 601–619.
[40] IUPAC-IUB Commission on Biochemical Nomenclature, J. Mol. Biol. 1970;52:1–17.

[41] J. Janin, S. Wodak, M. Levitt, B. Maigret, J. Mol. Biol. 125 (1978) 357–386.
[42] E. Benedetti, G. Morelli, G. Nemethy, H.A. Scheraga, Int. J. Pept. Protein Res. 22 (1983) 1–15.
[43] P.K. Ponnuswamy, V. Sasisekaran, Int. J. Pept. Protein Res. 3 (1971) 9–18.
[44] C. Ramakrishnan, N. Prasad, Int. J. Prot. Res. 3 (1971) 209–231.
[45] D.F. Stickle, L.G. Presta, K.A. Dill, G.D. Rose, J. Mol. Biol. 226 (1992) 1143–1159.
[46] C. Toniolo, CRC Crit. Rev. Biochem. 9 (1980) 1–44.
[47] S. Datta, N. Shamala, A. Banerjee, P. Balaram, J. Pept. Res. 49 (1997) 604–611.
[48] Type I β-turn, $(\phi_{i+1}, \psi_{i+1}) = (-60°, -30°)$, $(\phi_{i+2}, \psi_{i+2}) = (-90°, 0°)$: T.E. Creighton, in: Proteins: structures and molecular properties, 2nd ed., W.H. Freeman and Company, New York, 1993, pp. 226.
[49] R.S. Macomber, J. Chem. Educ. 69 (1992) 375–378.
[50] For 1:1 and 2:3 complexes, $K = [1{:}1\ CoCl_2\text{-peptide complex}]/[CoCl_2][\text{peptide ligand } (\mathbf{1})]$ and $[2{:}3\ CoCl_2\text{-peptide complex}]/[CoCl_2][\text{peptide ligand } (\mathbf{1})]^{3/2}$, respectively.
[51] Holzwarth, P. Doty, J. Am. Chem. Soc. 87 (1965) 218–228.
[52] M. Woody, R.W. Woody, Biopolymers 31 (1991) 569–586.
[53] C. Toniolo, A. Poleses, F. Formaggio, M. Crisma, J. Kamphuis, J. Am. Chem. Soc. 118 (1996) 2744–2745.
[54] C. Postmus, J.R. Ferrano, A. Quattorochi, K. Shobatake, K. Nakamoto, Inorg. Chem. 8 (1969) 1851–1855.
[55] K. Nakamoto, in: Infrared and Raman Spectra of Inorganic and Coordination Compounds, 4th ed., Wiley, New York, 1986, pp. 329.